

Department of Biomedical Sciences
University of Veterinary Medicine Vienna

Institute of Pharmacology and Toxicology
(Head: Univ.-Prof. Dr.med.univ. Veronika Sexl)

Tenascin-C Influences Vascular Dysfunction After Myocardial Infarction in Mice

Diploma Thesis
University of Veterinary Medicine Vienna

submitted by

Lukas Weber

Vienna, April 2020

Internal supervisor: Univ.-Prof. Dr.med.univ. Veronika Sexl
Institute of Pharmacology and Toxicology
Head: Univ.-Prof. Dr.med.univ. Veronika Sexl
University of Veterinary Medicine Vienna

External supervisors: Dr. med. univ. Patrick Michael Pilz &
Univ.-Prof. Dr. Bruno Podesser
Center for Biomedical Research
Head: Univ.-Prof. Dr. Bruno Podesser
Medical University of Vienna

Further Support (Center for Biomedical Research, Medical University of Vienna):

Attila Kiss, PhD

Petra Lujza Szabo, MSc.

Dr. med. Zsuzsanna Arnold

Eylem Acar

Milat Inci

Christopher Dostal

Valentina Budroni, MSc. (Max Perutz Labs)

Abstract

Background: Myocardial infarction (MI) is the result of a coronary artery occlusion and accounts for the highest number of deaths worldwide. The activation of the local and systemic renin-angiotensin-aldosterone system (RAAS) post MI is considered to play an important role in adverse cardiovascular remodeling. In addition, the extracellular matrix protein tenascin-C (TNC), was shown to be upregulated by angiotensin II in cardiomyocytes. This study aims to further investigate the crosstalk of TNC and the RAAS post MI as well as the role of TNC upregulation in vascular reactivity post MI.

Methods: Permanent ligation of the left anterior descending coronary artery was performed in male wildtype (WT) and TNC knockout (KO) mice to induce MI. Animals were sacrificed either one- or seven-days post MI, then lung, serum and parts of the thoracic aorta were taken for further analyses. Additionally, one group of WT mice was treated with TNC siRNA four days post MI to reduce TNC upregulation. Vascular reactivity was assessed in aortic ring segments using a wire myograph. In addition, TNC serum levels were measured using an ELISA kit and the activity of angiotensin-converting enzyme (ACE) was determined in lung and serum using a kinetic fluorescence assay.

Results: Contractile function in isolated aortic rings in exposure to the alpha 1 agonist phenylephrine was significantly higher in TNC KO mice compared to WT animals seven days post MI. TNC serum levels were significantly increased in WT mice one day post MI in comparison to non-infarcted control animals and high levels were maintained even seven days post MI. Finally, a trend of lower ACE activity in lungs of TNC KO mice could be found.

Conclusion: Lack of TNC preserves vascular contractile function. This indicates that TNC might play a pivotal role in vascular dysfunction post MI. Infarcted TNC KO mice also showed a tendency to lower ACE activity in lung tissue samples. These preliminary results further point out that TNC might be an important driver of post MI cardiac and vascular remodeling via a mechanism affecting ACE activity.

Zusammenfassung

Hintergrund: Der Myokardinfarkt (MI) als fatale Folge einer koronaren Gefäßerkrankung ist die häufigste Todesursache weltweit. Es konnte gezeigt werden, dass die Aktivierung des lokalen und systemischen Renin-Angiotensin-Aldosteron Systems (RAAS) eine entscheidende Rolle im adversen kardiovaskulären Remodeling nach MI spielt. Weiters wurde gezeigt, dass das extrazelluläre Matrixprotein Tenascin-C (TNC) in Anwesenheit von Angiotensin II hochreguliert wird. Unsere Studie zielte darauf ab, den Zusammenhang zwischen TNC und dem RAAS im Gefäßsystem nach MI weiter zu erforschen.

Methoden: Mittels permanenter Ligatur des *Ramus interventricularis anterior* der linken Koronararterie wurde in TNC Knockout- (KO) und Wildtyp- (WT) Mäusen ein MI induziert. Einen bzw. sieben Tage post MI wurden die Tiere sakrifiziert und Lungen, Serum sowie Anteile der thorakalen Aorta für weiterführende Untersuchungen entnommen. Zusätzlich wurde eine Gruppe von WT-Mäusen vier Tage post MI mit TNC-siRNA behandelt, um ein Knockdown der TNC Genexpression auszulösen. Die vaskuläre Reaktivität wurde durch Myograph-Messungen von Ringsegmenten der Aorta analysiert. TNC-Serumkonzentrationen wurden mittels ELISA-Kit bestimmt. Die Aktivität des Angiotensin-konvertierenden Enzyms (ACE) als Teil des RAAS, wurde anhand von kinetischen Fluoreszenzmessungen evaluiert.

Ergebnisse: Die kontraktile Funktion der Aorta in Zusammenhang mit dem alpha 1 Agonisten Phenylephrin war sieben Tage post MI signifikant besser in TNC KO-Tieren verglichen mit WT-Tieren. TNC-Serumkonzentrationen waren in WT-Mäusen bereits einen Tag post MI signifikant erhöht im Vergleich zu nicht-operierten Kontrolltieren und erhöhte TNC-Levels konnten auch noch sieben Tage post MI festgestellt werden. Außerdem zeigten TNC KO-Mäuse einen Trend zu niedrigerer pulmonaler ACE-Aktivität sieben Tage post MI.

Conclusio: Die Abwesenheit von TNC erhält die Kontraktionsfähigkeit von Aortensegmenten post MI. Dies lässt vermuten, dass TNC das vaskuläre Remodeling nach MI beeinflusst. Außerdem zeigten TNC KO Mäuse post MI einen Trend zu niedrigerer pulmonaler ACE-Aktivität. Diese Ergebnisse deuten darauf hin, dass TNC das kardiovaskuläre Remodeling nach MI durch eine Aktivierung des RAAS vorantreiben könnte.

Table of Contents

1. Introduction	1
1.1 Myocardial Infarction	1
1.1.2 Cardiovascular Remodeling After Myocardial Infarction	2
1.2 Tenascin-C	4
1.2.1 Tenascin-C in Cardiovascular Remodeling.....	4
1.3 The Role of the Renin-Angiotensin-Aldosterone System in Cardiovascular Remodeling	5
2. Hypothesis and Aims of the Study	8
3. Materials and Methods	9
3.1 Animal Groups and Timeline of Animal Experiments	9
3.2 Tenascin-C Knockout Mice	10
3.3 Mouse Model of Myocardial Infarction, Tenascin-C siRNA Treatment and Organ Harvesting.....	11
3.3.1 Left Anterior Descending Coronary Artery Ligation – Induction of Myocardial Infarction	11
3.3.2 Tenascin-C siRNA Treatment	12
3.3.3 Organ Harvesting	12
3.4 Vascular Reactivity Assessment in Aortic Rings	13
3.5 Determination of Tenascin-C Levels in Serum	14
3.6 Angiotensin-Converting Enzyme Activity Measurements	15
3.7 Statistical Analysis.....	15
4. Results	16
4.1 Organ and Body Weights.....	16
4.2 Vascular Reactivity.....	17
4.3 Tenascin-C Levels in Serum Samples	20

4.4 Angiotensin-Converting Enzyme Activity Measurements	21
5. Discussion.....	23
6. Conclusion.....	26
7. References	27

List of Tables

Table 1: Overview of animal groups, treatments, times of survival and animal numbers	9
Table 2: Body weight loss after surgery, heart weight/body weight ratio and lung weight/body weight ratio	16

List of Figures

Figure 1: Clinical classification of type 1 myocardial infarction	2
Figure 2: Overview of cardiac remodeling mechanisms after myocardial injury	3
Figure 3: Effects of angiotensin II on the different cell types involved in cardiovascular disease	6
Figure 4: Timeline of animal experiments.	10
Figure 5: Suture of the left anterior descending coronary artery	12
Figure 6: Ex vivo evaluation of infarcted heart area seven days after myocardial infarction ..	13
Figure 7: Organ bath chamber of the myograph.....	14
Figure 8: Wire myograph contractility assay of aortic segments	18
Figure 9: Wire myograph relaxation assay of aortic segments.	19
Figure 10: ELISA measurement of TNC serum levels in non-operated WT mice	20
Figure 11: Measurements of ACE activity in A: lung tissue lysates and B: serum	22

List of abbreviations

ACE	Angiotensin-converting enzyme
Ang I	Angiotensin I
Ang II	Angiotensin II
AT ₁ R	Angiotensin type 1 receptor
AT ₂ R	Angiotensin type 2 receptor
CVD	Cardiovascular disease
ECG	Electrocardiogram
ECM	Extracellular matrix
KO	Knock-out
LAD	Left anterior descending coronary artery
LV	Left ventricle
MI	Myocardial infarction
MMFK	Medetomidine midazolam fentanyl ketamine
MMPs	Matrix metalloproteinases
PMN	Polymorphonuclear leukocytes
RAAS	Renin-angiotensin-aldosterone system
RT	Room temperature
siRNA	Small interfering RNA
SNP	Sodium nitroprusside
SNS	Sympathetic nervous system
STEMI	ST-segment elevation myocardial infarction
TNF- α	Tumor necrosis factor α

TNC	Tenascin-C
VSMC	Vascular smooth muscle cells
WT	Wild type

1. Introduction

1.1 Myocardial Infarction

The ‘Global Burden of Disease Study’ showed that cardiovascular diseases (CVD) accounted for approximately 18 million deaths in 2015, therefore being the biggest contributor in mortality. Half of these deaths were attributed to ischemic heart disease of which myocardial infarction (MI) is the most severe form (Roth et al. 2017). In Austria in 2017, approximately 22% of all deaths were attributed to ischemic heart disease (Global Health Data Exchange. <http://ghdx.healthdata.org/gbd-results-tool> (accessed Mar 23, 2020)). Therefore, CVDs remain a major topic in medical research all around the world.

MI describes the death of cardiomyocytes due to ischemia in the myocardium. The disease was classified into 3 clinical types of which type 1 MI is the most common form and relevant for this thesis. In type 1 MI, ischemia is caused by rupture or erosion of an atherosclerotic plaque within a coronary artery (Figure 1). As a result, the affected coronary artery may be occluded or narrowed thus causing insufficient oxygen supply of the ventricular wall. Type 2 MI comprises all forms of MI that are not caused by atherosclerotic thrombi, e.g. coronary vasospasm, microvascular dysfunction and severe anemia. Finally, type 3 MI covers all cases showing symptoms of severe acute myocardial ischemia that cannot be further evaluated clinically because of precocious cardiac death (Thygesen et al. 2019).

MI can further be classified by different presentations of electrocardiogram (ECG) tracing. About 36% of clinically manifest MIs present ST-segment elevation (STEMI) which accounts for total occlusion of a coronary artery and transmural infarction (i.e. affecting all layers of the ventricular wall).

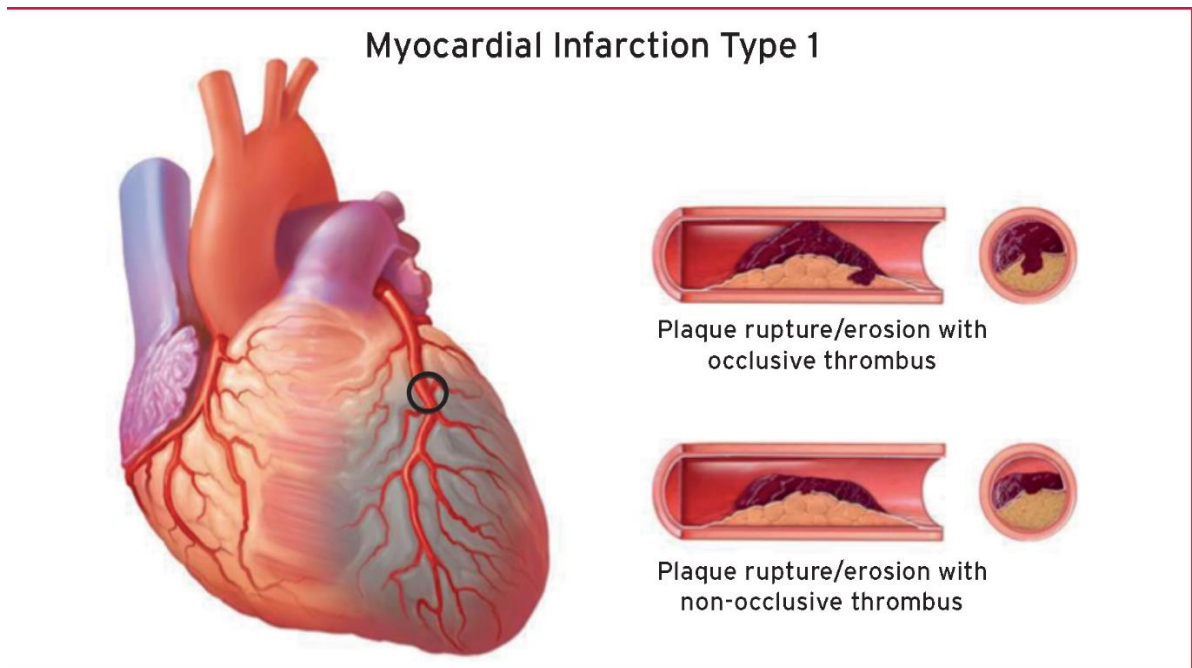


Figure 1: Clinical classification of type 1 myocardial infarction (Thygesen et al. 2019).

1.1.2 Cardiovascular Remodeling After Myocardial Infarction

The occurring pathophysiological remodeling mechanisms within the ventricle after MI are still not entirely understood. These mechanisms post MI can be distinguished in early and late phase remodeling (Figure 2). The early changes within the infarcted heart comprise the infiltration of inflammatory cells such as polymorphonuclear leukocytes (PMN), the activation of matrix metalloproteinases (MMP) and its associated tissue inhibitors (TIMP) and the subsequent changes within the extracellular matrix (ECM), which are caused by MMPs. While these early changes lead to left ventricle (LV) dilation and wall thinning, they are important to remove and replace the infarcted tissue, thus maintaining cardiac function. Later, fibroblasts contribute to the formation of scar tissue by depositing collagen within the extracellular space. There is substantial evidence that the release of neurohormones (e.g. vasopressin, epinephrine) is triggering the activation of the sympathetic nervous system (SNS) and the renin-angiotensin-aldosterone system (RAAS) and thereby play a role in LV remodeling (Bhatt et al. 2017).

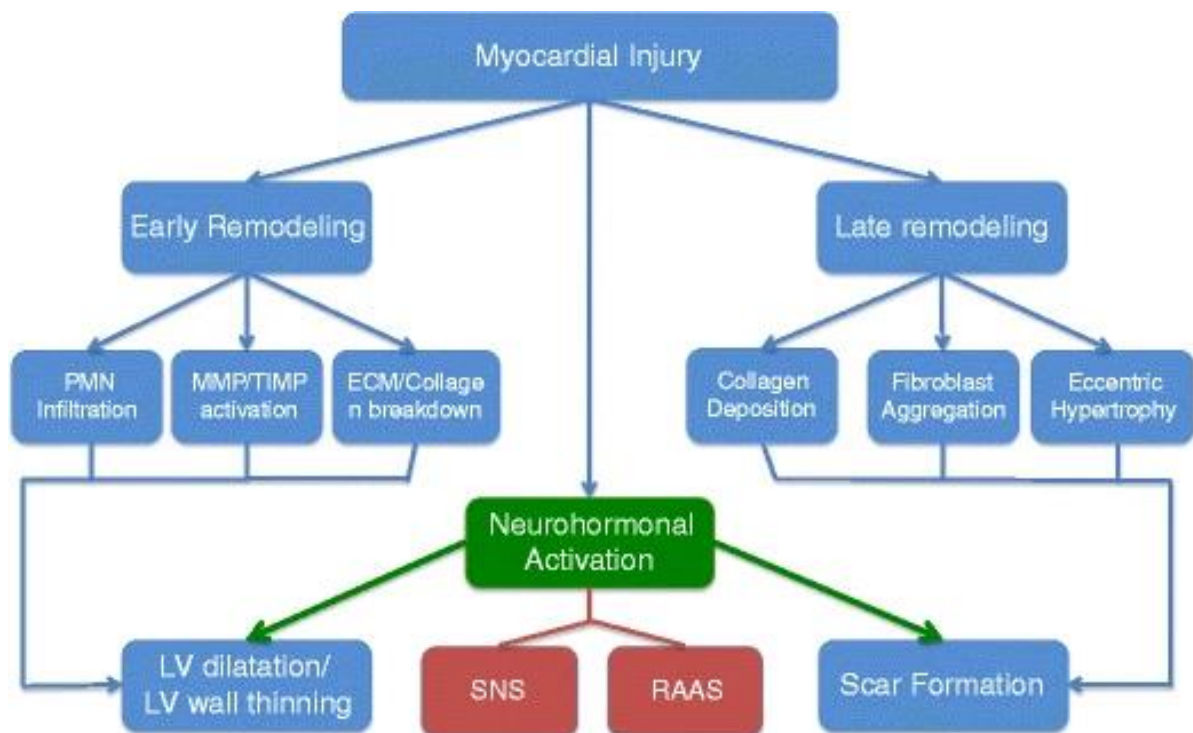


Figure 2: Overview of cardiac remodeling mechanisms after myocardial injury. ECM, extracellular matrix; LV, left ventricle; MMP, matrix metalloproteinase; PMN, polymorphonuclear leukocyte; RAAS, renin-angiotensin-aldosterone system; SNS, sympathetic nervous system; TIMP, tissue inhibitor of metalloproteinase (Bhatt et al. 2017).

Especially the product of ACE, angiotensin II (Ang II) contributes to these adverse remodeling processes such as fibrosis, LV dysfunction and dilatation. More recently, our group demonstrated for the first time that cardiomyoblasts incubated with Ang II markedly increased the expression of the ECM protein tenascin-C (TNC) (Gonçalves et al. 2019). TNC was shown to be expressed abundantly within the border zone between healthy and infarcted cardiac tissue and upregulation of TNC was also associated with worse clinical outcome after acute MI (Frangogiannis 2017, Sato et al. 2012). However, the causative role of TNC in cardiac and vascular remodeling following MI is largely unknown.

1.2 Tenascin-C

Tenascin-C (TNC) is a glycoprotein of the ECM. It was first described in the 1980s as an important factor in fetal neuronal development and in oncogenesis of mammary tumors (Chiquet-Ehrismann et al. 1986). In adults, however, it could only be found in stem cell niches (bones) and in association with inflammation, injury and solid tumors (Brösicke and Faissner 2015, Chiquet-Ehrismann et al. 2014, Midwood et al. 2011).

Current research focuses mainly on the role of TNC in remodeling and concomitant fibrosis. Accordingly, in a mouse model of skin and lung fibrosis it has been shown recently that TNC drives fibrosis involving Toll-like receptor 4 (TLR4) signaling (Bhattacharyya et al. 2016). Similarly to these findings, another study showed that TNC is a part of the fibrogenic niche in renal fibrosis in a mouse model of kidney dysfunction (Fu et al. 2017).

Recently, immunomodulatory properties of TNC have been evaluated. Macrophage polarization through TLR4 signaling was shown to be of high importance in remodeling mechanisms after MI. TNC KO mice showed less LV remodeling and increased presence of anti-inflammatory M2-macrophages, thus indicating that these cell subsets might ameliorate post MI remodeling (Kimura et al. 2019).

1.2.1 Tenascin-C in Cardiovascular Remodeling

As mentioned above, TNC as a part of the ECM plays an important role in early remodeling after myocardial injury (Figure 2). It was shown that TNC is overexpressed in the border zone and infarcted zone after MI. In addition, TNC KO mice subjected to MI showed significantly less fibrosis and preserved LV function, suggesting the pathophysiological importance of TNC in LV remodeling post MI (Nishioka et al. 2010).

Another study in rats showed that TNC was highly expressed by epicardium-derived cells post MI. These epicardial progenitor cells are normally inactive within adult hearts but were found to be reactivated in response to myocardial injury. TNC also showed to support the migration of these cells within the ECM (Hesse et al. 2017).

The most prevalent cause of MI is atherosclerosis that affects the coronary arteries. Interestingly, TNC is known to be involved in the pathogenesis of atherosclerosis. In 1999, increased expression of TNC in human atherosclerotic plaques was shown (Wallner et al. 1999). More recently, a clinical study revealed that patients with increased TNC serum levels developed a higher risk of rupturing coronary artery plaques (Sakamoto et al. 2014).

Moreover, our group demonstrated that a lack of TNC preserved cardiac function and decreased the amount of fibrosis and hypertrophy in a mouse model of chronic pressure overload, confirming the adverse role of TNC in LV remodeling (Podesser et al. 2018).

Besides the importance in LV remodeling, some studies pointed out the pathophysiological importance of TNC in vascular diseases such as intimal hyperplasia and calcification (Vyavahare et al. 2000, Yamamoto et al. 2005).

1.3 The Role of the Renin-Angiotensin-Aldosterone System in Cardiovascular Remodeling

As mentioned above, the RAAS is activated by neurohormones after myocardial injury (Figure 2) and contributes to adverse ventricular remodeling by affecting vascular smooth muscle cells (VSMCs), endothelial cells, cardiac cells and the ECM (*Figure 3*) (Mehta and Griendling 2007).

Ang II is the central effector molecule of the RAAS. It derives from angiotensinogen that is converted to angiotensin I (Ang I) by the proteinase renin. Finally, Ang I is cleaved to Ang II by angiotensin-converting enzyme (ACE) (Patel et al. 2017). The major sources of ACE are endothelial cells of the lung and epithelial cells of the kidney tubules (Erdös 1976). Ang II increases blood pressure through vasoconstriction and renal water retention.

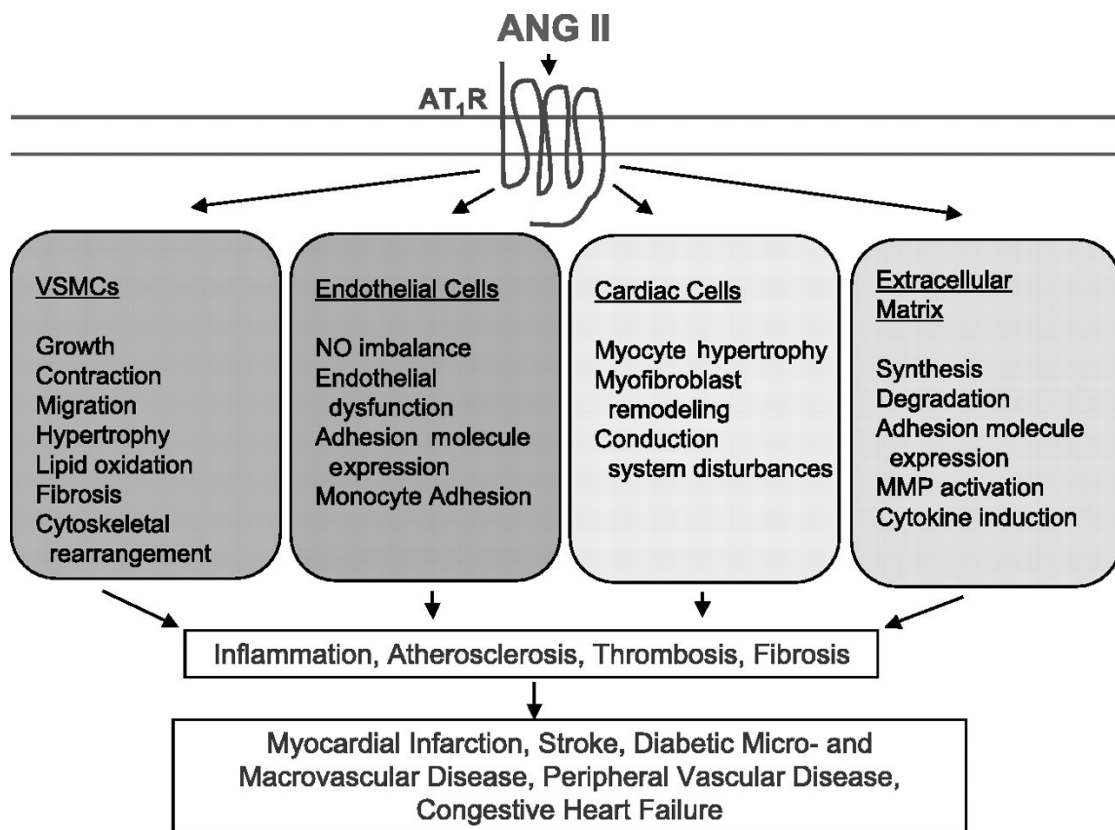


Figure 3: Effects of angiotensin II on the different cell types involved in cardiovascular disease (Mehta and Griendling 2007).

Long term activation of Ang II leads to hypertrophy of VSMCs, thus contributing to the development of vascular dysfunction (Geisterfer et al. 1988). More recent studies showed that other cell types are also affected by Ang II: Arenas *et al.* demonstrated that Ang II triggered endothelial cells to secrete MMP-2 and tumor necrosis factor α (TNF- α), thus contributing to endothelial dysfunction and inflammation (Arenas et al. 2004). Another study showed the direct influence of Ang II on cardiomyocytes as cardiac hypertrophy could be prevented through blockade of angiotensin type 1 receptor (AT₁R) (Kim et al. 1995). Apart from the effect of Ang II on cardiomyocytes and cardiac fibroblasts, Ang II signaling also directly promotes vascular remodeling and subsequent contractile and relaxation dysfunction by affecting endothelial cells and VSMCs (Forrester et al. 2018).

Finally, the ECM also played an important role in Ang II-induced cardiovascular remodeling: Ang II did not only promote collagen synthesis through AT₁R but also through the angiotensin type 2 receptor (AT₂R) (Mifune et al. 2000).

AT₁R blockers and ACE inhibitors are the most frequently used therapeutics in the treatment of CVD. Apart from lowering blood pressure, these drugs are also known to ameliorate conditions as atherosclerosis, diabetes and endothelial dysfunction (Henriksen et al. 2001, Igarashi et al. 2001, Schiffrin et al. 2000). ACE inhibitors did not only show to attenuate ventricular remodeling by reducing Ang II levels, they also significantly reduced MMP-2 activity in a model of chronic volume overload (Brower et al. 2007).

2. Hypothesis and Aims of the Study

In this study, we aimed to investigate the potential contribution of TNC in the progression of peripheral (aorta) vascular dysfunction following MI. We hypothesized that an upregulation of TNC after MI would lead to impaired vascular reactivity by affecting ACE activity. Furthermore, we conducted a pilot study using TNC siRNA as a possible treatment option to prevent both vascular and cardiac dysfunction post MI.

Therefore, we performed a permanent ligation of the left anterior descending coronary artery (LAD) in mice to induce transmural MI. We used this model to investigate concomitant effects of MI on 1) the expression of the ECM protein TNC, 2) the activation of the RAAS and 3) vascular reactivity.

3. Materials and Methods

3.1 Animal Groups and Timeline of Animal Experiments

Animal experiments were approved by the animal ethics commission of the Medical University of Vienna and the Federal Ministry of Education, Science and Research of Austria (Geschäftszahl: BMBWF-66.009/0224-V/3b/2019). The severity of the animal procedures was classified as ‘severe’. Male WT and TNC KO mice of the inbred strain A/J were used in this study. Mice were taken for surgery with a weight of 20-25 g (age 6 to 11 weeks) and randomly assigned to one of the six different groups, as listed below (Table 1). MI was induced by permanent ligation of the LAD.

Table 1: Overview of animal groups, treatments, times of survival and animal numbers

	Group name	Surgery and treatment	Time of survival (days)	Number of animals (n)
1	WT Baseline	no	7	3
2	WT MI 1d	LAD ligation	1	11
3	WT SHAM 7d	SHAM surgery	7	2
4	WT MI 7d	LAD ligation	7	10
5	WT MI TNC siRNA treatment	LAD ligation, TNC siRNA treatment 4 days post MI	7	4
6	TNC KO MI 7d	LAD ligation	7	2

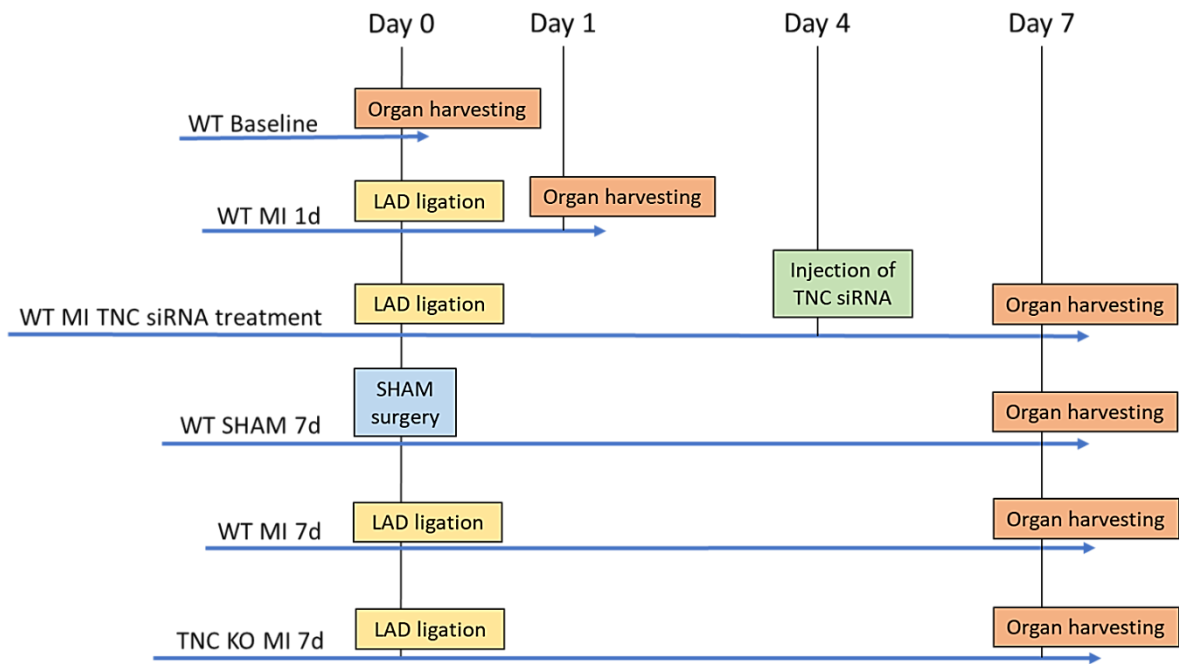


Figure 4: Timeline of animal experiments. Animals were divided into six different groups, which were subjected to different operations and treatments. At day 0, all groups were subjected to either LAD ligation (WT MI 1d, WT MI TNC siRNA treatment, WT MI 7d, TNC KO MI 7d), SHAM surgery (WT SHAM 7d) or no surgery (WT baseline) and organs were harvested at given time points. Additionally, WT MI TNC siRNA received a single injection of TNC siRNA at day 4.

3.2 Tenascin-C Knockout Mice

Homozygous male TNC KO mice (A/J.Cg-Tnc^{tm1Sia}/Rbrc) were generated as described previously (Saga et al. 1992) and backcrossed with the inbred strain A/J (The Jackson Laboratory, Bar Harbor, Maine, USA) for twenty generations. Male WT A/J mice were taken as control animals.

3.3 Mouse Model of Myocardial Infarction, Tenascin-C siRNA Treatment and Organ Harvesting

3.3.1 Left Anterior Descending Coronary Artery Ligation – Induction of Myocardial Infarction

The LAD ligation was performed as described previously by Santer *et al.* (Santer et al. 2015). Mice were anesthetized by a single s.c. injection of MMFK solution (0.3 mg/kg medetomidine, 1 mg/kg midazolam, 0.03 mg/kg fentanyl, 10 mg/kg ketamine). After intubation, animals were permanently ventilated with a mixture of ambient air and oxygen during the whole surgical procedure. Animals were placed in a supine position on a heating pad with permanent ECG surveillance through needle probes attached to their limbs. The surgery was performed using an OP microscope. The left side of the thorax was shaved and disinfected. The skin was incised and after replacing the muscles, thoracotomy was performed by opening the fourth intercostal space. At this point, the left auricle as well as the LV wall were well visible. However, the LAD was not visible since it is lying profoundly within the ventricular wall. The pericardium was opened and removed. The heart stitch was performed approximately 2 mm below the left auricle using a 7-0 prolene suture and fixed with 5-6 knots (Figure 5). Correct positioning of the suture was proven immediately by sudden paling of the LV and remarkable ST – elevation in the ECG (STEMI). In case of SHAM-surgery the heart was punctured but afterwards the suture material was removed, and no LAD ligation was performed. After successful LAD ligation/SHAM-surgery, residual air within the thorax was removed by increasing the adjusted tidal volume while closing the thorax. After closing thorax and skin the animals were brought into a prone position. In order to awake the mice, an antidote of MMFK (1 mg/kg atipamezole, 0.1 mg/kg flumazenil) was injected s.c. As soon as they showed first signs of awaking, they were extubated, and the ECG electrodes were removed. To improve post OP recovery, mice were administered 0.5 ml glucose solution s.c. For post-operative analgesia, mice received buprenorphine (0.12 mg/kg, s.c.) as soon as they started to move normally again. Furthermore, mice received piritramide through drinking water *ad libitum* (15 mg piritramide and 10 ml of 10% glucose in 250 ml water) for the first three days after surgery.

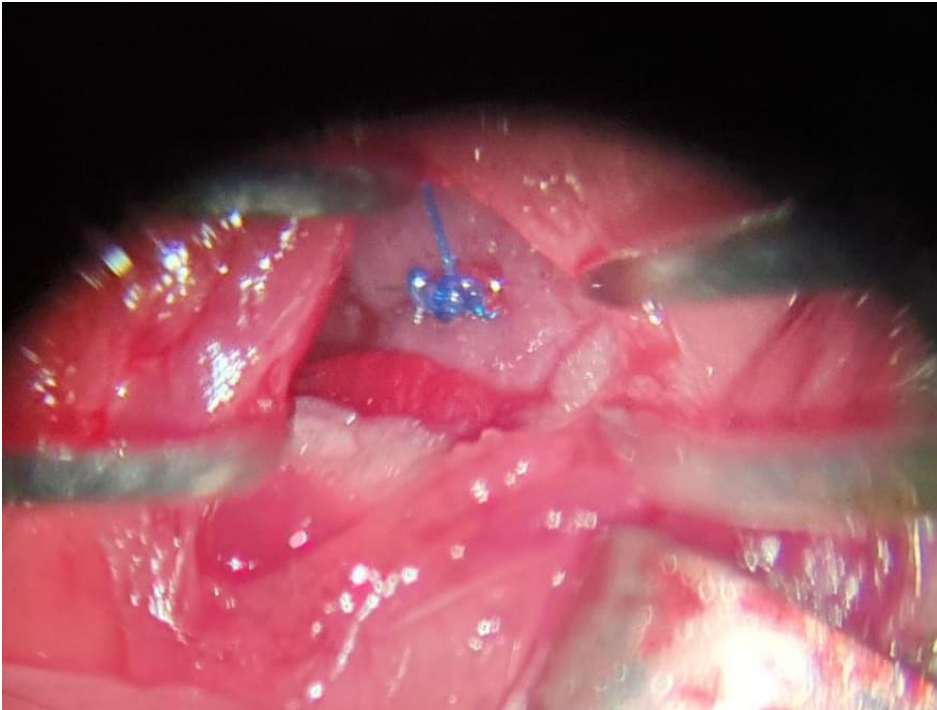


Figure 5: Suture of the left anterior descending coronary artery visualized through an OP microscope (Photo: Attila Kiss)

3.3.2 Tenascin-C siRNA Treatment

On day four after LAD ligation one group of WT mice was transfected with TNC siRNA to induce a knockdown of TNC gene expression, as described previously (Fu et al. 2017). In brief, a suspension of 100 μ g TNC siRNA (Tenascin-C siRNA (h): sc-43186, Santa Cruz Biotechnology, Inc.) was prepared using an *in vivo*-jetPEI® kit (Polyplus-transfection, Inc.) and mice received a single bolus i.p. injection.

3.3.3 Organ Harvesting

Mice were anesthetized with an overdose of MMFK and put in a supine position. Sternum and parts of the ribs were removed to gain full sight of heart and lungs. Blood was taken from the caudal vena cava with a 1 ml syringe then heart and lungs were removed, weighed and shock-frozen in liquid nitrogen. Correct positioning of the LAD suture was verified after excision of the heart by checking the infarcted area under a stereomicroscope (Figure 6). Finally, a large

part of the thoracic aorta was excised and directly taken for the wire myograph assay (see ‘Vascular Reactivity Assessment in Aortic Rings’ below).



Figure 6: Ex vivo evaluation of infarcted heart area seven days after myocardial infarction using a stereomicroscope (Photo: Christopher Dostal).

3.4 Vascular Reactivity Assessment in Aortic Rings

For these measurements we used aortic ring segments in a DMT wire myograph system. After excision of the thoracic aorta the vessel was directly put in Krebs solution (NaCl 130 mM, KCl 4.7 mM, KH_2PO_4 1.18 mM, MgSO_4 7 mM, H_2O 1.17 mM, NaHCO_3 14.9 mM, Glucose 5.5 mM, EDTA 0.026 mM, CaCl_2 1.6 mM). Surrounding tissue of the vessels were removed under a stereo microscope and segments of approx. 2 mm length were mounted onto the hooks (Figure 7). First, we assessed maximum contractility by adding high potassium Krebs solution (124 mM KCl) to the organ bath. The reactivity to KCl solution gives us information about the overall

viability of the vessel, by causing depolarization and therefore contraction of the VSMCs. Afterwards the KCl solution was washed out and the vessel was put into Krebs buffer solution to regain physiological status of contractility. Then the aortic ring was constricted using increasing dosages of phenylephrine solution (10^{-9} M to 10^{-6} M). Phenylephrine is a sympathomimetic drug that acts on alpha-1 receptors of VSMCs. After having evaluated contractile function we proceeded with measuring endothelium-dependent vasorelaxation. Therefore, acetylcholine concentrations (10^{-9} M to 10^{-5} M) were increased within the organ bath. Acetylcholine acts on muscarinic acetylcholine receptors of the endothelial cells, thus inducing endothelium-dependent vasorelaxation. Finally, endothelium-independent relaxation was determined by applying sodium nitroprusside (SNP) (10^{-10} M to 10^{-6} M).



Figure 7: Organ bath chamber of the myograph with 200 μ m hooks installed, after mounting an aortic segment (Photo: Christopher Dostal)

3.5 Determination of Tenascin-C Levels in Serum

TNC serum levels were measured by using an Elabscience Sandwich-ELISA kit, according to the manufacturer's instructions. In brief, 10 μ L of serum were diluted in 90 μ L PBS and incubated within the ELISA plate for 90 min at 37°C. Afterwards the biotinylated detection antibody was added and again incubated for 60 min. After following incubation with

horseradish peroxidase for 30 min the substrate agent was added to the wells for 15 min. The enzyme-substrate reaction was blocked by adding a stop-solution and TNC serum levels were measured using a plate reader at a wavelength of 450 nm.

3.6 Angiotensin-Converting Enzyme Activity Measurements

ACE activity was measured in both lung and serum samples by using a kinetic fluorescence assay as described before (Fagyas et al. 2014). In brief, lungs were lysed, homogenized and centrifuged at 13000 rpm for 5 min. The total protein content of the lysates was determined using a PierceTM BCA Protein Assay Kit. The tissue homogenates were then diluted to a protein concentration of 1 mg/ml each. Using a black 96 well microplate, 6 μ l of tissue homogenate or serum were diluted in 100 mM TRIS buffer, 50 mM NaCl and 10 μ M ZnCl₂ with 15 μ M Abz-FRK(Dnp)P-OH substrate (synthesized by Peptide 2.0, Chantilly, VA, USA) to gain a total volume of 210 μ l per well. The intensity of fluorescence was measured in a plate reader at 37°C and wavelengths of λ_{ex} =340 nm and λ_{em} =405 nm.

3.7 Statistical Analysis

All data were analyzed using GraphPad Prism 8 software (Version 8.4.0). For multiple comparisons a one-way ANOVA and post-hoc tests were used. Values were presented as mean \pm standard deviation. Differences between groups were considered as statistically significant with P-values of less than 0.05.

4. Results

4.1 Organ and Body Weights

Animals were weighed before surgery and on the day of organ harvest to determine post MI body weight loss. Moreover, hearts and lungs were weighed after excision to determine heart weight/body weight ratio and lung weight/body weight ratio (Table 2).

Table 2: Body weight loss after surgery, heart weight/body weight ratio and lung weight/body weight ratio. Data presented as mean values with SD. * $p < 0.05$.

	Group name	Number of animals (n)	Body weight loss after surgery (%)	Heart weight/body weight ratio (%)	Lung weight/body weight ratio (%)
1	WT Baseline	3	no surgery	0.43 ± 0.02 *	0.57 ± 0.03
2	WT MI 1d	11	6.14 ± 2.9	0.48 ± 0.03	0.71 ± 0.22
3	WT SHAM 7d	2	1.45 ± 4.06	0.42 ± 0.03	0.57 ± 0.01
4	WT MI 7d	10	3.55 ± 3.72	0.50 ± 0.04 *	0.69 ± 0.18
5	WT MI TNC siRNA treatment	4	16.03 ± 11.07	0.53 ± 0.08	0.63 ± 0.08
6	TNC KO MI 7d	2	6.50 ± 5.20	0.55 ± 0.04	0.97 ± 0.31

Significant differences could only be found in the heart weight/body weight ratios between non-infarcted control animals ('WT Baseline') and infarcted WT mice seven days post MI ('WT MI 7d'). This finding confirms that MI leads to an increase of the heart weight/body weight ratio in WT mice.

4.2 Vascular Reactivity

The overarching aim of this study was to determine whether TNC has an impact on peripheral (aorta) vascular function following MI. Accordingly, vascular contractility and relaxation properties were determined in isolated aortic ring preparations.

First, we investigated the function of VSMCs using an aortic ring contractility assay (Figure 8). The assay was performed in the groups 'WT MI 7d', 'TNC KO MI 7d' and 'WT MI TNC siRNA treatment' to determine whether the single injection of TNC siRNA affected the vascular reactivity. The measurements using KCl showed that infarcted TNC KO animals produced higher contraction response compared to WT and TNC siRNA groups (Figure 8, A). However, these findings did not reach statistical significance.

Next, we investigated the contractile response using the alpha 1 adrenergic receptor agonist phenylephrine. We demonstrated that TNC KO mice showed significantly higher contractions in comparison to WT MI and TNC siRNA groups (TNC KO MI 7d: 10.64 ± 1.50 mN; WT MI 7d: 5.63 ± 1.70 mN; WT MI TNC siRNA treatment: 4.33 ± 1.35 mN; $p < 0.01$) (Figure 8, B).

These findings may suggest that lack of TNC preserves vascular contractile function and prevents long-term vascular stiffness. Notably, this effect was not detectable in the animals that received TNC siRNA treatment on day 4 post MI, thus indicating this process may initiate at an earlier time point (1-3 days) after MI.

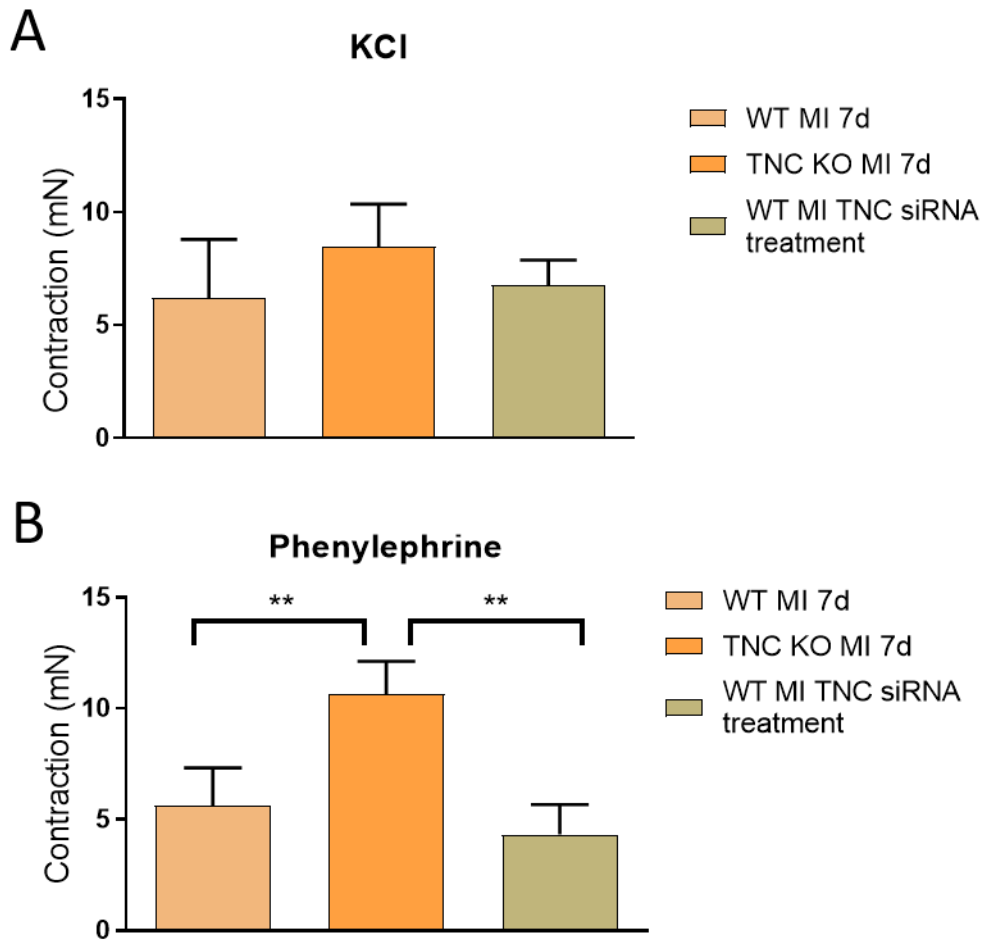


Figure 8: Wire myograph contractility assay of aortic segments 7 days post MI in WT mice (WT MI 7d; $n = 5$), TNC KO mice (TNC KO MI 7d; $n = 2$) and mice that received a single injection of TNC siRNA 4 days post MI (WT MI TNC siRNA treatment; $n = 4$). Aortic segments were incubated with A: KCl solution (124 mM) or B: phenylephrine solution (1 μ M). Data presented as mean values with SD. $**p < 0.01$

Vascular endothelial function was assessed by applying a cumulative dosage of acetylcholine in isolated vessel rings. No significant differences were found in the endothelium-dependent (acetylcholine) relaxation assay (Figure 9, A). Similarly, the endothelium-independent vasorelaxation (triggered by the application of sodium nitroprusside (SNP)) did not show any differences between the groups (Figure 9, B).

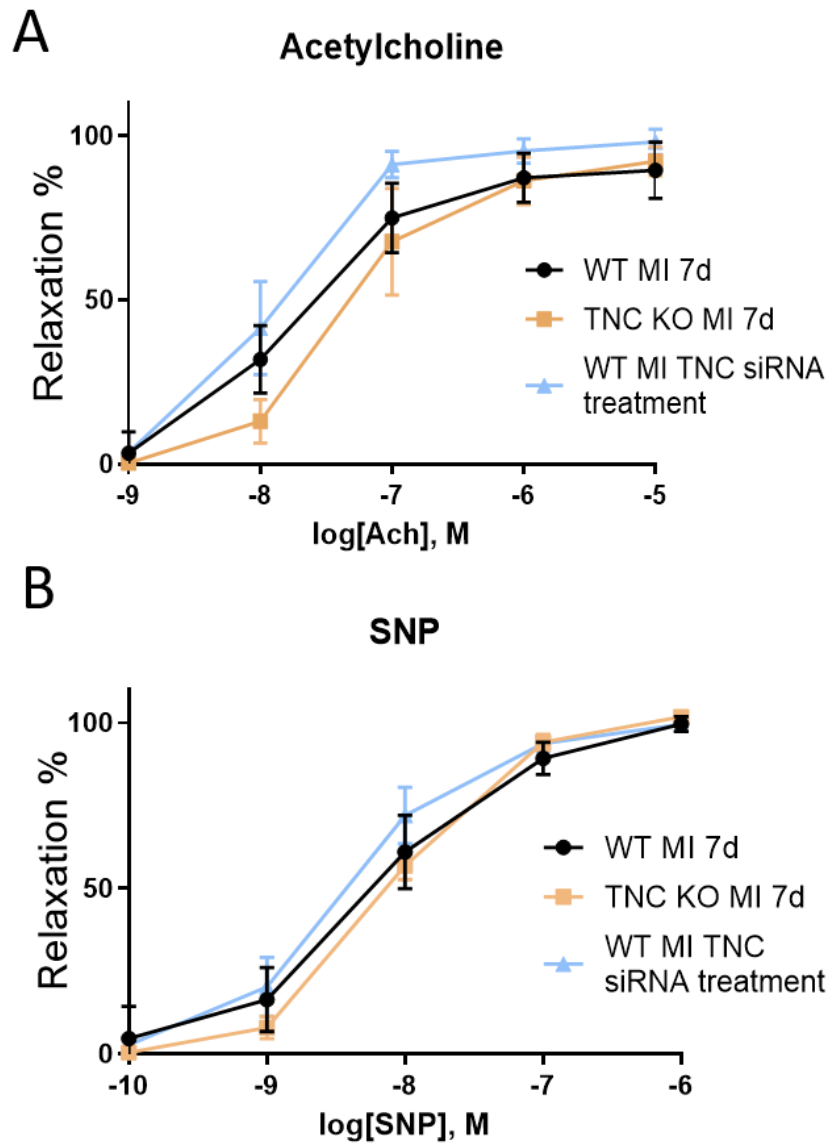


Figure 9: Wire myograph relaxation assay of aortic segments 7 days post MI in WT mice (WT MI 7d; $n = 5$), TNC KO mice (TNC KO MI 7d; $n = 2$) and mice that received a single injection of TNC siRNA 4 days post MI (WT MI TNC siRNA treatment; $n = 4$). Aortic segments incubated with A: acetylcholine (concentration increasing from 10^{-9} M to 10^{-5} M) or B: sodium nitroprusside (SNP) (concentration increasing from 10^{-10} M to 10^{-6} M). Mean values with SD.

Collectively, we found significant differences in contractile function between TNC KO mice and WT mice seven days post MI (Figure 8, B), indicating that lack of TNC might prevent adverse adaptations in vascular contractility. Conversely, this effect could not be seen in the group that received a TNC siRNA treatment at day 4 post MI.

4.3 Tenascin-C Levels in Serum Samples

A previous study of the Podesser lab showed that plasma levels of TNC were significantly increased post MI (Gonçalves et al. 2019). However, it has not been investigated at which timepoint TNC protein levels would reach their maximum post MI. Therefore, we compared serum samples of mice which were sacrificed at day 1 and 7 post MI. Furthermore, we aimed to investigate if the TNC siRNA treatment four days post MI could significantly lower TNC serum levels on day seven post MI (Figure 10).

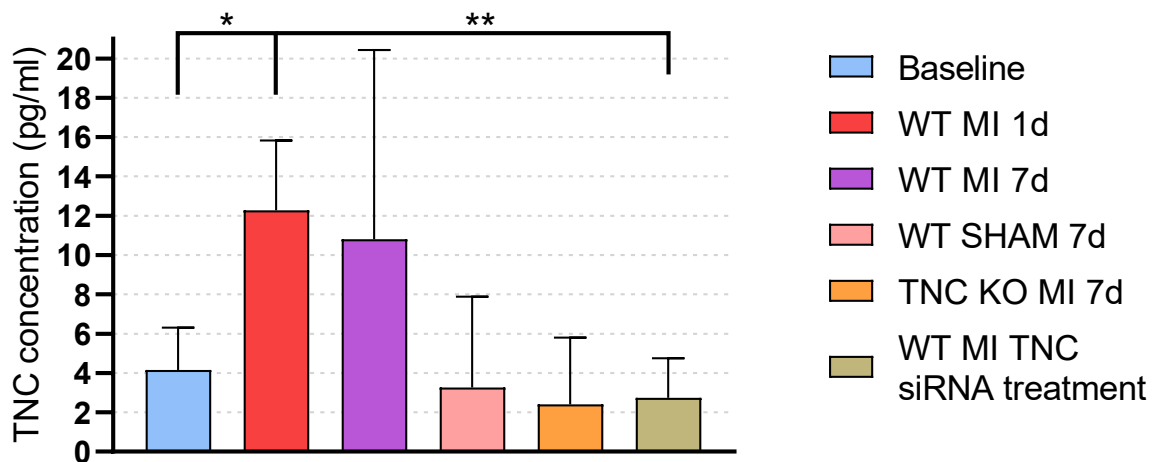


Figure 10: ELISA measurement of TNC serum levels in non-operated WT mice (Baseline; $n = 3$), WT mice 1 day post MI (WT MI 1d; $n = 7$), 7 days post-MI (WT MI 7d; $n = 7$) SHAM operated WT mice (WT SHAM 7d; $n = 2$), TNC KO mice 7 days post-MI (TNC KO MI 7d; $n = 2$), WT mice treated with a single TNC siRNA injection 4 days after MI and serum taken 7 days post-MI (WT MI TNC siRNA treatment; $n = 4$). Mean values with SD. * $p < 0.05$, ** $p < 0.01$

TNC serum levels of infarcted WT mice one day post MI were approximately four times higher than levels of SHAM, TNC KO and TNC siRNA-treated animals. Due to low animal numbers and high variance of TNC serum levels within the groups, statistical significance could only be shown in infarcted WT animals one day post MI versus non-operated control animals (WT MI 1d: 12.28 ± 3.54 pg/ml vs. Baseline: 4.16 ± 2.16 pg/ml; $p < 0.05$) and between ‘WT MI 1d’ (12.28 ± 3.54 pg/ml) and ‘WT MI TNC siRNA treatment’ (2.75 ± 2.01 pg/ml) ($p < 0.01$) (Figure 10).

These results showed that increased protein expression of TNC occurs within 24 hours after induction of MI. In addition, we observed lower TNC serum levels (to the same extent as TNC KO mice) in animals that received a single injection of TNC siRNA four days after infarction compared to WT animals, which showed abundant TNC expression on day 1 and 7 post MI. This confirmed the efficacy of the TNC siRNA transfection.

4.4 Angiotensin-Converting Enzyme Activity Measurements

Besides the evaluation of vascular reactivity and TNC serum levels, we investigated whether TNC affected the activity of ACE in lung and serum samples (Figure 11).

In lung samples of TNC KO mice, we found a tendency to lower ACE activity in comparison to infarcted WT mice (Figure 11, A). This tendency was not presented in TNC siRNA-treated mice (Figure 11, A). In addition, there was no difference in ACE activity in serum samples between the groups (Figure 11, B)

These results showed that there was a trend of lower ACE activity in lungs of infarcted TNC KO mice in comparison to infarcted WT mice.

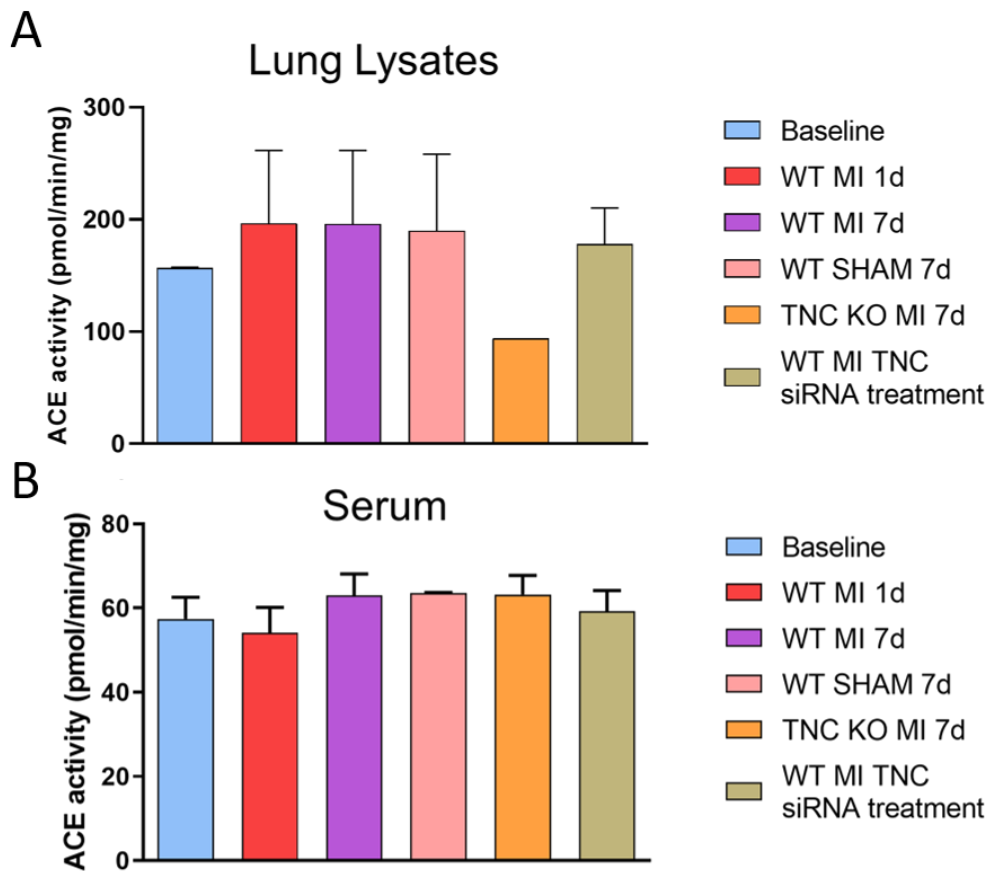


Figure 11: Measurements of ACE activity in *A*: lung tissue lysates and *B*: serum, determined by a fluorescent kinetic assay. Non-operated WT mice (Baseline; *A*: $n = 2$, *B*: $n = 3$), WT mice 1 day post MI (WT MI 1d; $n = 11$), WT mice 7 days post MI (WT MI 7d; *A*: $n = 8$, *B*: $n = 10$), SHAM operated WT mice (WT SHAM 7d; $n = 2$), TNC KO mice 7 days post-MI (TNC KO MI 7d; *A*: $n = 1$, *B*: $n = 2$), WT mice treated with a single TNC siRNA injection 4 days after MI and organs taken 7 days post-MI (WT MI TNC siRNA treatment; $n = 4$). Mean values with SD.

5. Discussion

Vascular stiffness and endothelial dysfunction are independent factors for future cardiovascular events. Both are accelerated following acute MI and subsequently may increase the risk for additional atherothrombotic events. In this study, we aimed to enlighten the role of TNC in cardiac and vascular dysfunction post MI. Previously, it has been described that TNC drives adverse LV remodeling in a rat model of MI (Gonçalves et al. 2019). However, the influence of TNC on peripheral vascular function after MI has not been investigated yet. Therefore, we used a wire myograph methodological approach to assess VSMC and endothelial function in isolated aortic rings from WT and TNC KO mice subjected to MI. In detail, VSMC function was assessed by measuring vascular contractility, and endothelial function was analyzed by measuring vasorelaxation using various compounds. Furthermore, we for the first time performed an *in vivo* transfection with TNC siRNA to induce a knockdown of TNC expression and subsequently characterized cardiac and vascular function. To confirm the efficacy of the TNC siRNA treatment, we measured TNC levels in serum samples by ELISA. Finally, we evaluated ACE activity in lungs and serum samples to investigate the potential interaction between TNC and the activation of RAAS in post MI adverse remodeling.

The most important findings were that infarcted WT mice showed significantly lower contractile function of aortic segments in exposure to the alpha 1 agonist phenylephrine than infarcted TNC KO mice, suggesting the impact of TNC on vascular function and remodeling after MI (Figure 8, B). These findings were in line with previous studies that showed TNC-dependent fibrosis and vascular calcification, thus causing stiffness of the affected vessels (Nishioka et al. 2010, Vyavahare et al. 2000). We believe that TNC affects vascular dysfunction via different signaling cascades (integrin or TLR4). Previous studies also highlighted the pathophysiological importance of TNC in various CVDs such as atherosclerosis and Kawasaki disease (Wang et al. 2018, Yokouchi et al. 2019). However, these studies demonstrated the expression of TNC in the affected vessels, whereas in our study we did not look at TNC expression within the aorta after MI.

Of importance, we observed that TNC serum levels were increased already one day post MI and maintained high levels even seven days post MI (Figure 10). Our results also pointed out

that the decline in response to phenylephrine-induced vasoconstriction is certainly an early mechanism in peripheral vascular beds, since the TNC siRNA application on day 4 post MI was not able to reverse the contractile function (Figure 8). However, we acknowledge the limitation of low animal numbers in the TNC KO group and admit that more animals are needed to gain a reliable conclusion. Nevertheless, we suggest that the pathophysiological changes within the VSMCs might develop already within the first four days after MI since they could not be reversed by a systemic knockdown of TNC starting on day 4 post MI. In order to confirm this, a follow-up study with another cohort of animals should be performed: WT mice should be treated with siRNA 1) immediately after induction of MI and 2) 24 hours after infarction. Then, vascular reactivity should be assessed after seven days to evaluate if this treatment could preserve VSMC function. Furthermore, the expression of TNC within the vessels and in cardiomyocytes will be assessed by immunohistochemical stainings.

Besides the contractile function, we also performed experiments in order to characterize the role of TNC in endothelium-dependent and endothelium-independent vasorelaxation in aortic segments (Figure 9). Acetylcholine induces vasorelaxation through an endothelium-dependent mechanism, therefore giving us information about the viability of endothelial cells. We found no significant differences between groups. Collectively, our data suggest preserved endothelial function through the TNC siRNA treatment in the early phase of post MI remodeling. Further studies are warranted to clarify the long-term effects and the potential role of TNC in endothelial dysfunction post MI.

Next, we investigated the potential interaction of ACE and TNC. In a previous study of our lab we found that Ang II, the product of ACE, markedly increased the expression of TNC in H9c2 cardiomyoblasts (Gonçalves et al. 2019). In addition, unpublished data of our group demonstrated that TNC KO mice under chronic pressure overload resulted in less LV dilation and cardiac fibrosis in association with lower cardiac ACE activity, compared to WT mice. In the current study, we measured ACE activity in serum and lung samples. We observed a tendency to increased ACE activity in lung tissue of infarcted WT mice while TNC KO mice showed a decline in ACE activity (Figure 11, A). Subsequently, we suggest that less ACE activity in lungs and therefore decreased activation of Ang II in TNC KO mice may explain the preserved vascular function. However further studies are needed to confirm this assumption. In

addition, the levels of ACE activity in lungs of TNC siRNA-treated animals were similar to the WT MI groups, suggesting the very early time point interaction between ACE and TNC following MI (Figure 11, A). We suggest that a lack of TNC decelerates the activation of ACE in lungs and therefore subsequently decreases the production of Ang II, thereby mitigating cardiac and vascular adverse remodeling following MI.

In the serum samples, we could not find any differences between the groups (Figure 11, B). This is not surprising since previous studies demonstrated that ACE is mainly present in endothelial cells, fibroblasts and inflammatory cells (after infiltration into the damaged tissue) (Bernstein et al. 2018). Therefore, our next steps are 1) to isolate fibroblasts and cardiomyocytes of infarcted mice and 2) to measure the expression and activity of ACE within these cells.

6. Conclusion

To conclude, our findings showed that contractile function of the thoracic aorta segments was preserved in TNC KO mice seven days post MI compared to WT animals (Figure 8, B). Moreover, we established a protocol to attenuate TNC expression post MI by siRNA *in vivo* transfection. Accordingly, WT mice treated with TNC siRNA (on day 4 post MI) showed significantly less TNC expression in serum samples seven days post MI (Figure 10). However, this transfection could not reverse ACE activity and vascular contractile function.

To sum up, TNC may be a critical mediator in the progression of cardiovascular dysfunction as well as a potential therapeutic target in post MI remodeling. Therefore, local TNC silencing at an early timepoint post MI might be a promising treatment option.

7. References

- Arenas IA, Xu Y, Lopez-Jaramillo P, Davidge ST. 2004. Angiotensin II-induced MMP-2 release from endothelial cells is mediated by TNF-alpha. *American journal of physiology. Cell physiology*, 286 (4): C779-84. DOI 10.1152/ajpcell.00398.2003.
- Bernstein KE, Khan Z, Giani JF, Cao D-Y, Bernstein EA, Shen XZ. 2018. Angiotensin-converting enzyme in innate and adaptive immunity. *Nature reviews. Nephrology*, 14 (5): 325–336. DOI 10.1038/nrneph.2018.15.
- Bhatt AS, Ambrosy AP, Velazquez EJ. 2017. Adverse Remodeling and Reverse Remodeling After Myocardial Infarction. *Current cardiology reports*, 19 (8): 71. DOI 10.1007/s11886-017-0876-4.
- Bhattacharyya S, Wang W, Morales-Nebreda L, Feng G, Wu M, Zhou X, Lafyatis R, Lee J, Hinchcliff M, Feghali-Bostwick C, Lakota K, Budinger GRS, Raparia K, Tamaki Z, Varga J. 2016. Tenascin-C drives persistence of organ fibrosis. *Nature communications*, 7: 11703. DOI 10.1038/ncomms11703.
- Brösicke N, Faissner A. 2015. Role of tenascins in the ECM of gliomas. *Cell adhesion & migration*, 9 (1-2): 131–140. DOI 10.1080/19336918.2014.1000071.
- Brower GL, Levick SP, Janicki JS. 2007. Inhibition of matrix metalloproteinase activity by ACE inhibitors prevents left ventricular remodeling in a rat model of heart failure. *American journal of physiology. Heart and circulatory physiology*, 292 (6): H3057-64. DOI 10.1152/ajpheart.00447.2006.
- Chiquet-Ehrismann R, Mackie EJ, Pearson CA, Sakakura T. 1986. Tenascin: an extracellular matrix protein involved in tissue interactions during fetal development and oncogenesis. *Cell*, 47 (1): 131–139. DOI 10.1016/0092-8674(86)90374-0.
- Chiquet-Ehrismann R, Orend G, Chiquet M, Tucker RP, Midwood KS. 2014. Tenascins in stem cell niches. *Matrix biology : journal of the International Society for Matrix Biology*, 37: 112–123. DOI 10.1016/j.matbio.2014.01.007.
- Erdös EG. 1976. Conversion of angiotensin I to angiotensin II. *The American Journal of Medicine*, 60 (6): 749–759. DOI 10.1016/0002-9343(76)90889-5.

- Fagyas M, Úri K, Siket IM, Daragó A, Boczán J, Bányai E, Édes I, Papp Z, Tóth A. 2014. New perspectives in the renin-angiotensin-aldosterone system (RAAS) I: endogenous angiotensin converting enzyme (ACE) inhibition. *PloS one*, 9 (4): e87843. DOI 10.1371/journal.pone.0087843.
- Forrester SJ, Booz GW, Sigmund CD, Coffman TM, Kawai T, Rizzo V, Scalia R, Eguchi S. 2018. Angiotensin II Signal Transduction: An Update on Mechanisms of Physiology and Pathophysiology. *Physiological reviews*, 98 (3): 1627–1738. DOI 10.1152/physrev.00038.2017.
- Frangogiannis NG. 2017. The extracellular matrix in myocardial injury, repair, and remodeling. *The Journal of clinical investigation*, 127 (5): 1600–1612. DOI 10.1172/JCI87491.
- Fu H, Tian Y, Zhou L, Zhou D, Tan RJ, Stolz DB, Liu Y. 2017. Tenascin-C Is a Major Component of the Fibrogenic Niche in Kidney Fibrosis. *Journal of the American Society of Nephrology : JASN*, 28 (3): 785–801. DOI 10.1681/ASN.2016020165.
- Geisterfer AA, Peach MJ, Owens GK. 1988. Angiotensin II induces hypertrophy, not hyperplasia, of cultured rat aortic smooth muscle cells. *Circulation research*, 62 (4): 749–756. DOI 10.1161/01.res.62.4.749.
- Gonçalves IF, Acar E, Costantino S, Szabo PL, Hamza O, Tretter EV, Klein KU, Trojanek S, Abraham D, Paneni F, Hallström S, Kiss A, Podesser BK. 2019. Epigenetic modulation of tenascin C in the heart: implications on myocardial ischemia, hypertrophy and metabolism. *Journal of hypertension*, 37 (9): 1861–1870. DOI 10.1097/HJH.0000000000002097.
- Henriksen EJ, Jacob S, Kinnick TR, Teachey MK, Krekler M. 2001. Selective angiotensin II receptor antagonism reduces insulin resistance in obese Zucker rats. *Hypertension (Dallas, Tex. : 1979)*, 38 (4): 884–890. DOI 10.1161/hy1101.092970.
- Hesse J, Leberling S, Boden E, Friebe D, Schmidt T, Ding Z, Dieterich P, Deussen A, Roderigo C, Rose CR, Floss DM, Scheller J, Schrader J. 2017. CD73-derived adenosine and tenascin-C control cytokine production by epicardium-derived cells formed after myocardial infarction. *FASEB journal : official publication of the*

- Federation of American Societies for Experimental Biology, 31 (7): 3040–3053.
DOI 10.1096/fj.201601307R.
- Igarashi M, Hirata A, Yamaguchi H, Tsuchiya H, Ohnuma H, Tominaga M, Daimon M, Kato T. 2001. Candesartan inhibits carotid intimal thickening and ameliorates insulin resistance in balloon-injured diabetic rats. *Hypertension (Dallas, Tex. : 1979)*, 38 (6): 1255–1259. DOI 10.1161/hy1101.095537.
- Kim S, Ohta K, Hamaguchi A, Yukimura T, Miura K, Iwao H. 1995. Angiotensin II induces cardiac phenotypic modulation and remodeling in vivo in rats. *Hypertension (Dallas, Tex. : 1979)*, 25 (6): 1252–1259. DOI 10.1161/01.hyp.25.6.1252.
- Kimura T, Tajiri K, Sato A, Sakai S, Wang Z, Yoshida T, Uede T, Hiroe M, Aonuma K, Ieda M, Imanaka-Yoshida K. 2019. Tenascin-C accelerates adverse ventricular remodeling after myocardial infarction by modulating macrophage polarization. *Cardiovascular research*, 115 (3): 614–624. DOI 10.1093/cvr/cvy244.
- Mehta PK, Griendling KK. 2007. Angiotensin II cell signaling: physiological and pathological effects in the cardiovascular system. *American journal of physiology. Cell physiology*, 292 (1): C82-97. DOI 10.1152/ajpcell.00287.2006.
- Midwood KS, Hussenet T, Langlois B, Orend G. 2011. Advances in tenascin-C biology. *Cellular and molecular life sciences : CMLS*, 68 (19): 3175–3199.
DOI 10.1007/s00018-011-0783-6.
- Mifune M, Sasamura H, Shimizu-Hirota R, Miyazaki H, Saruta T. 2000. Angiotensin II type 2 receptors stimulate collagen synthesis in cultured vascular smooth muscle cells. *Hypertension (Dallas, Tex. : 1979)*, 36 (5): 845–850. DOI 10.1161/01.hyp.36.5.845.
- Nishioka T, Onishi K, Shimojo N, Nagano Y, Matsusaka H, Ikeuchi M, Ide T, Tsutsui H, Hiroe M, Yoshida T, Imanaka-Yoshida K. 2010. Tenascin-C may aggravate left ventricular remodeling and function after myocardial infarction in mice. *American journal of physiology. Heart and circulatory physiology*, 298 (3): H1072-8.
DOI 10.1152/ajpheart.00255.2009.
- Patel S, Rauf A, Khan H, Abu-Izneid T. 2017. Renin-angiotensin-aldosterone (RAAS): The ubiquitous system for homeostasis and pathologies. *Biomedicine & pharmacotherapy*

= *Biomedecine & pharmacotherapie*, 94: 317–325.

DOI 10.1016/j.biopha.2017.07.091.

Podesser BK, Kreibich M, Dzilic E, Santer D, Förster L, Trojanek S, Abraham D, Krššák M, Klein KU, Tretter EV, Kaun C, Wojta J, Kapeller B, Gonçalves IF, Trescher K, Kiss A. 2018. Tenascin-C promotes chronic pressure overload-induced cardiac dysfunction, hypertrophy and myocardial fibrosis. *Journal of hypertension*, 36 (4): 847–856.

DOI 10.1097/HJH.0000000000001628.

Roth GA, Johnson C, Abajobir A, Abd-Allah F, Abera SF, Abyu G, Ahmed M, Aksut B, Alam T, Alam K, Alla F, Alvis-Guzman N, Amrock S, Ansari H, Ärnlöv J, Asayesh H, Atey TM, Avila-Burgos L, Awasthi A, Banerjee A, Barac A, Bärnighausen T, Barregard L, Bedi N, Belay Ketema E, Bennett D, Berhe G, Bhutta Z, Bitew S, Carapetis J, Carrero JJ, Malta DC, Castañeda-Orjuela CA, Castillo-Rivas J, Catalá-López F, Choi J-Y, Christensen H, Cirillo M, Cooper L, Criqui M, Cundiff D, Damasceno A, Dandona L, Dandona R, Davletov K, Dharmaratne S, Dorairaj P, Dubey M, Ehrenkranz R, El Sayed Zaki M, Faraon EJA, Esteghamati A, Farid T, Farvid M, Feigin V, Ding EL, Fowkes G, Gebrehiwot T, Gillum R, Gold A, Gona P, Gupta R, Habtewold TD, Hafezi-Nejad N, Hailu T, Hailu GB, Hankey G, Hassen HY, Abate KH, Havmoeller R, Hay SI, Horino M, Hotez PJ, Jacobsen K, James S, Javanbakht M, Jeemon P, John D, Jonas J, Kalkonde Y, Karimkhani C, Kasaeian A, Khader Y, Khan A, Khang Y-H, Khera S, Khoja AT, Khubchandani J, Kim D, Kolte D, Kosen S, Krohn KJ, Kumar GA, Kwan GF, Lal DK, Larsson A, Linn S, Lopez A, Lotufo PA, El Razek HMA, Malekzadeh R, Mazidi M, Meier T, Meles KG, Mensah G, Meretoja A, Mezgebe H, Miller T, Mirrakhimov E, Mohammed S, Moran AE, Musa KI, Narula J, Neal B, Ngalesoni F, Nguyen G, Obermeyer CM, Owolabi M, Patton G, Pedro J, Qato D, Qorbani M, Rahimi K, Rai RK, Rawaf S, Ribeiro A, Safiri S, Salomon JA, Santos I, Santric Milicevic M, Sartorius B, Schutte A, Sepanlou S, Shaikh MA, Shin M-J, Shishehbor M, Shore H, Silva DAS, Sobngwi E, Stranges S, Swaminathan S, Tabarés-Seisdedos R, Tadele Atnafu N, Tesfay F, Thakur JS, Thrift A, Topor-Madry R, Truelsen T, Tyrovolas S, Ukwaja KN, Uthman O, Vasankari T, Vlassov V, Vollset SE, Wakayo T, Watkins D, Weintraub R, Werdecker A, Westerman R, Wiysonge CS, Wolfe C, Workicho A, Xu G, Yano Y, Yip P, Yonemoto

- N, Younis M, Yu C, Vos T, Naghavi M, Murray C. 2017. Global, Regional, and National Burden of Cardiovascular Diseases for 10 Causes, 1990 to 2015. *Journal of the American College of Cardiology*, 70 (1): 1–25. DOI 10.1016/j.jacc.2017.04.052.
- Saga Y, Yagi T, Ikawa Y, Sakakura T, Aizawa S. 1992. Mice develop normally without tenascin. *Genes & development*, 6 (10): 1821–1831. DOI 10.1101/gad.6.10.1821.
- Sakamoto N, Hoshino Y, Misaka T, Mizukami H, Suzuki S, Sugimoto K, Yamaki T, Kunii H, Nakazato K, Suzuki H, Saitoh S-i, Takeishi Y. 2014. Serum tenascin-C level is associated with coronary plaque rupture in patients with acute coronary syndrome. *Heart and vessels*, 29 (2): 165–170. DOI 10.1007/s00380-013-0341-2.
- Santer D, Nagel F, Kreibich M, Dzilic E, Moser PT, Muschitz G, Inci M, Krssak M, Plasenzotti R, Bergmeister H, Trescher K, Podesser BK. 2015. In vivo and ex vivo functional characterization of left ventricular remodelling after myocardial infarction in mice. *ESC heart failure*, 2 (3): 171–177. DOI 10.1002/ehf2.12039.
- Sato A, Hiroe M, Akiyama D, Hikita H, Nozato T, Hoshi T, Kimura T, Wang Z, Sakai S, Imanaka-Yoshida K, Yoshida T, Aonuma K. 2012. Prognostic value of serum tenascin-C levels on long-term outcome after acute myocardial infarction. *Journal of cardiac failure*, 18 (6): 480–486. DOI 10.1016/j.cardfail.2012.02.009.
- Schiffrin EL, Park JB, Intengan HD, Touyz RM. 2000. Correction of arterial structure and endothelial dysfunction in human essential hypertension by the angiotensin receptor antagonist losartan. *Circulation*, 101 (14): 1653–1659. DOI 10.1161/01.cir.101.14.1653.
- Thygesen K, Alpert JS, Jaffe AS, Chaitman BR, Bax JJ, Morrow DA, White HD. 2019. Fourth universal definition of myocardial infarction (2018). *European heart journal*, 40 (3): 237–269. DOI 10.1093/eurheartj/ehy462.
- Vyavahare N, Jones PL, Tallapragada S, Levy RJ. 2000. Inhibition of Matrix Metalloproteinase Activity Attenuates Tenascin-C Production and Calcification of Implanted Purified Elastin in Rats. *The American journal of pathology*, 157 (3): 885–893. DOI 10.1016/S0002-9440(10)64602-0.

- Wallner K, Li C, Shah PK, Fishbein MC, Forrester JS, Kaul S, Sharifi BG. 1999. Tenascin-C is expressed in macrophage-rich human coronary atherosclerotic plaque. *Circulation*, 99 (10): 1284–1289. DOI 10.1161/01.cir.99.10.1284.
- Wang Z, Wei Q, Han L, Cao K, Lan T, Xu Z, Wang Y, Gao Y, Xue J, Shan F, Feng J, Xie X. 2018. Tenascin-c renders a proangiogenic phenotype in macrophage via annexin II. *Journal of cellular and molecular medicine*, 22 (1): 429–438. DOI 10.1111/jcmm.13332.
- Yamamoto K, Onoda K, Sawada Y, Fujinaga K, Imanaka-Yoshida K, Shimpo H, Yoshida T, Yada I. 2005. Tenascin-C is an essential factor for neointimal hyperplasia after aortotomy in mice. *Cardiovascular research*, 65 (3): 737–742. DOI 10.1016/j.cardiores.2004.10.034.
- Yokouchi Y, Oharaseki T, Enomoto Y, Sato W, Imanaka-Yoshida K, Takahashi K. 2019. Expression of tenascin C in cardiovascular lesions of Kawasaki disease. *Cardiovascular pathology : the official journal of the Society for Cardiovascular Pathology*, 38: 25–30. DOI 10.1016/j.carpath.2018.10.005.